



NUMERICAL INVESTIGATION OF MODIFIED SAVONIUS WIND TURBINE WITH VARIOUS STRAIGHT BLADE ANGLE

Khairil Anwar^{1,2*}, Syukri Himran², Luther Sule², Nasruddin Azis²

¹Department of Mechanical Engineering – Tadulako University, Palu, Indonesia

²Department of Mechanical Engineering – Hasanuddin University, Makassar, Indonesia

*Corresponding Author email: khairilanwar@untad.ac.id; khairilannwars@gmail.com

This is an open access article distributed under the Creative Commons Attribution License, which permits unrestricted use, distribution, and reproduction in any medium, provided the original work is properly cited.

ARTICLE DETAILS

Article History:

Received 23 May 2018

Accepted 24 September 2018

Available online 27 September 2018

ABSTRACT

The present paper aims to numerically investigate the two-dimensional flow analysis of modified Savonius wind turbine using computational fluid dynamics. The effects of the straight blade angle on the turbine performance were studied. Simulations based on the RANS equations and the SST-k- ω turbulence model are used to simulate the airflow over the turbine blades. Both the static and dynamic simulations were performed. In the static simulation, the drag and lift coefficient on the Savonius turbine were directly calculated at every angular position, and the time-averaged moment and power coefficients were computed in each of the dynamic simulations. From the results, it can be concluded that the turbine with a straight blade angle of 100° model gives the better performance at higher Tip Speed Ratio (TSR) than other models.

KEYWORDS

VAWT, Savonius wind turbine, Bach type, Computational Fluid Dynamics, Straight blade angle, Power Coefficient.

1. INTRODUCTION

The Savonius wind turbine is a mechanical power-generating device that has been studied by many researchers since the 1920s. This turbine has some advantages such as relatively simple construction, low manufacturing cost, wind reception from any direction with low operating speed, good starting ability and has many rotor configuration options. However, the efficiency of the Savonius wind turbines is lower than the other horizontal axis wind turbines due to the negative torque generated by the returning blade. Savonius wind turbines are usually applied as wind pump for irrigation or agricultural purposes, street lighting systems, and driving electrical generators [1-4].

Numerous experimental and numerical studies of the Savonius wind turbine have been found in many technical and scientific literatures. Different configurations and arrangements of Savonius rotor show that the rotor performance is influenced by operational conditions, geometric and airflow parameters. The performance of this rotor can be improved by changes in design parameters, including blade arc angle, aspect ratio, overlap size, and gap size [5-10]. The overlap and gap region between Savonius blades, allowing the fluid was entering the concave side of a blade to flow to the side of the other blades and produce additional pressure. Several studies about Savonius rotor have been carried out on the number of blades and stages of the rotor [11-16]. Some authors also have reported that augmentation and wind guide improve on power coefficient, that made the construction of the turbine system more complex [17-22]. Some studies of Savonius rotor focus on the modification of blade shape get better performance than the previous model. Published results demonstrate that Savonius rotor performance is affected by model and configuration of Savonius rotor [23-28].

The Savonius blade can be classified into three geometric shapes, classical or semicircular type, elliptical type, and Bach type. Bach type has a blade shape that is not entirely curved, but there is a section with a straight blade. A number of studies have found that, the Bach-type rotor is better than other geometries and modifying blade geometry has experimentally been shown to improve the performance of Bach type. Modi and Fernando conducted an experimental study and flow visualization on this Bach type

blade to get the best performance on the optimal configuration of the Savonius rotor associated with the blade geometry, gap size (a/d) = 0; blade overlap (b/d) = 0; aspect ratio (A) = 0.77; blade shape parameters (p/q) = 0.2; blade arc angle (ϕ) = 135° [29]. A group researchers performed the experiments by modifying the Bach-type blades without using a shaft, where $C_{p,max}$ was obtained on the blade with an overlap ratio of 0, the angle of the blade curve of 124° and the aspect ratio 0.7, compared with the semi-circular model [30]. Additionally, compared the new profile blade with modified Bach type, semi-circular blade, semi-elliptic blade, and Benesh type models to determine the optimum values of power coefficient. The optimized results obtained a new profile that performs better with $C_{p,max}$ 0.31 than modified Bach, Benesh type, semi-elliptic and semi-circular of 0.3; 0.29; 0.26 and 0.23 respectively.

Computational approaches have also been used to efficiently predict the flow past a Bach-type turbine and calculate its power coefficient. Wang and Yeung simulated the flow past a micro-scale Bach-type vertical-axis wind using a viscous Discrete-Vortex Method for use as micro-scale energy harvesters that can be applied to power [31]. A studied the flow physics around a modified Bach and Benesh profiles of Savonius rotor using multi-physics CFD solver to determine drag and lift characteristics acting on the rotors [32]. The result shows that the drag coefficient (CD) for the modified Bach profile is higher than the Benesh profile. Also, numerically analyzed three geometries of Savonius wind turbine rotors (semi-circular, elliptic and Bach type) [33]. All geometries attain maximum C_p at TSR 0:8. In that region, the Bach-type geometry produces the highest power output. Furthermore, the numerical investigation to assess an optimal blade profile in the modified design of Bach-type blades has been done, the results showed that the maximum power coefficient with blade arc angle of 135° [34].

The literature review reported presents that changes in the blade geometry design of Savonius wind turbines could improve the power coefficient. Many inventive design enhancements have been done on Bach-type blades, but the simplest modification is to modify the shape of the blade. Most of the previous research work carried out on modifications of the curved blade, relating to the arc angle of the blade for efficiency improvement, but the effect of straight blade angles on the performance of

the rotor has not been investigated so far. This straight blade is necessary to the movement of the airflow after passing through the curved blade leading to overlap areas which potentially reduces the negative torque of the returning blade. This section can be further investigated by bending the blade at the connection of the curved blade and the straight blade, inward and outward to form a specific angle.

In this paper, the main purpose of this study is to numerically investigate different modified Bach-type of savonius wind turbine configurations that differ for the bend angle between curved blade and straight blade to obtain optimum performance. Both dynamic and static simulations are executed. The static analyses are carried out to compute aerodynamic performance associated with lift and drag coefficients and the dynamic simulations to obtain turbine performance in terms of moment coefficient (C_M) and power coefficient (C_P) during operative cycles.

2. METHODOLOGY

2.1 Blade Model

This study focuses on the modification of the geometry of the Savonius wind turbine of Bach type, especially on the straight blade. The blade of the Savonius-Bach type as the baseline model used refers to Roy and Saha [34]. The optimum configuration is obtained at the angle of the blade curve $\phi = 135^\circ$, the length of the straight blade (S1) and the radius of the blade (S2) of 42% of the length of the blade chord, the blade overlap, $e = 40\%$ of the blade chord length and the distance between the blades, $a = 10\%$ of the blade chord length. Modify geometric shapes in which the straight blades are bent inwards and outward to form an angle (β) varied between of 70° - 110° at intervals of 10° (in this case, $\beta = 90^\circ$ is baseline or without being bent). The constant parameters are the rotor diameter (D), the blade angle (ϕ), the length of the straight blade (S1), the radius of the blade (S2) and, and the distance between the blades (a). The diagram of the modified design under test is shown in Fig. 1.

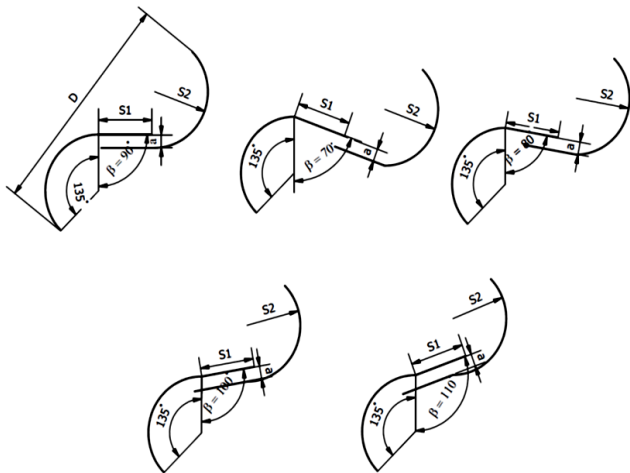


Figure 1: Geometry changes of Bach type blade at the different angle of β

2.2 Solution Methodology

In this study, the performance of Savonius wind turbine with straight blade modification was performed by numerical simulation using 2 (two) Dimensional Computational Fluid Dynamics for static and dynamic simulations. The static simulation is used to analyze the fluid flow characteristics across the blade at various angular positions, meanwhile dynamic simulation with rotating blades is used to predict the turbine performance with the parameters including power coefficient (C_P) and torque or moment coefficient (C_M). A total of 35 dynamic simulations were performed to calculate

$$TSR = \frac{\omega \cdot R}{V}$$

average C_M and averaged C_P , and 35 static simulations to determine the lift coefficient (C_L) and drag coefficient (C_D) during the half cycle of the turbine rotation due to symmetrical geometry. For dynamic simulation, a specific rotation rate N (rad/s) is determined to obtain variations in the tip speed ratio (TSR). Tip speed ratio indicates the ratio of blade tip speed to the wind velocity, and has the following expression:

where: ω is the turbine rotational speed; R is the rotor radius of rotation; V is the freestream velocity. The power coefficient C_P , the moment coefficient C_M , and the tip speed ratio TSR are as follows:

$$C_P = C_M \cdot TSR$$

The inlet velocity is taken 7 m/s for all simulations, with Reynolds number of 1.2×10^5 . The flow is assumed to be unsteady and turbulent, operating at a constant rotational rate for each case. Computational models are arranged in Gambit software, while numerical analysis is conducted with CFD Fluent. Figure 2 shows a two-dimensional model prepared in Gambit.

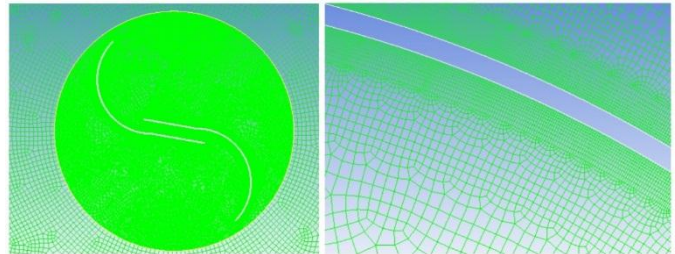


Figure 2: Mesh generation around the Savonius blade

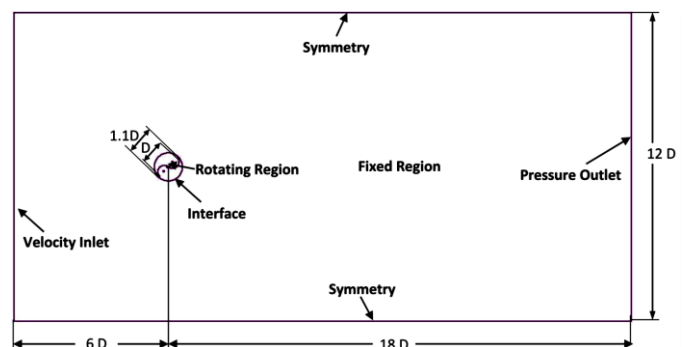


Figure 3: Boundary conditions and computational domain

The computational domain of rectangular shape shown in figure 3, dimensions are given based on turbine diameter. It is expected that the fluid flow passing through the turbine is not disturbed by the upper and lower sides of the domain. There are two regions in the computational domain: the rotating region of the turbine blades and the fixed areas on the outside, connected by the interfaces. The circle interfaces were made between the rotating and fixed region. The interface of the two mesh region boundaries have the same size, move against each other with no gaps to reduce calculation errors, and to achieve faster convergence.

The domain boundaries consist of the inlet velocity (the inlet side), the pressure outlet (the outlet side), and the top and bottom wall as symmetry. The no-slip boundary conditions are applied to the turbine blades. The domain is discretized using quadrilateral mesh. A size function was applied with the rotor blade to obtain the better computational results near the blade surface, with start size parameter was chosen 0.1 mm, the growth rate of 1.1 and size limit was 1 mm. In order to accurately capture the flow behaviour around the blades, ten boundary layers of the structural mesh were generated. The number of cells for the blade is about 178,000.

For the simulation process used 2D double precision assuming transient flow, the turbulent flow of the fluid is modelled by the Transition $k-\omega$ Shear Stress Transport (SST) turbulence model with low Reynolds corrections. The turbulent intensity of 1% and turbulent length scale of 0.01 was applied to approximately account for the incoming flow turbulence. The cell zone condition for dynamic simulation used mesh motion on the rotating domain by input rotational velocity to get the variation of tip speed ratio from 0.2 to 1.4. The solution method includes; (1) the Pressure-Velocity coupling with Semi-Implicit Method for Pressure-Linked Equations (SIMPLE); (2) the spatial discretization for pressure with second order, for momentum, turbulent kinetic energy, and specific dissipation rate with the second order upwind scheme to achieve accurate results; and (3) the transient formulation with second order implicit. For calculation, the number of time step 0.001 with 20 iterations per time step is used. The simulation was considered to have converged when the residuals of all conserved variables are below 1×10^{-5} .

3. RESULT AND DISCUSSION

3.1 Validation

Validation of simulation was performed using experimental data obtained from SANDIA Laboratories [35]. To verify the simulation parameters used in this simulation, turbine geometry was simulated under the same experimental test [35]. The semi-circular blade contained a full 180 arc with a radius, r , of 0.25 m, the dimensionless gap width, s/d , of 0.1 and the radius of the rotor, R , of 0.4762 m (configuration No.11), with the test Reynolds number of 4.32×10^5 . Two-dimensional transient simulations using the SST $k-\omega$ turbulence model have performed at various TSR. The averaged value of moment coefficient (C_M) generated from simulations. Figure 4 shows the comparison of moment Coefficients as a function of Tip Speed Ratio (TSR) between the experimental data and numerical result. The numerical results indicate the conformity of the experimental tests, at low to medium rotational speeds, using these simulation parameters. However, it can be observed that the difference between numerical simulations and the experimental data grows with the increase of the TSR. At very high rotational speeds and wind velocities, the flow separation occurs, which is a limiting characteristic of $k-\omega$ model [36].

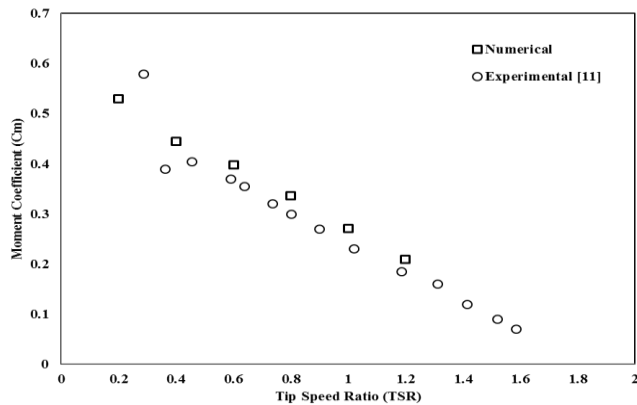


Figure 4: Moment Coefficient as a function of Tip Speed Ratio for numerical validation

3.2 Static Simulations

The study was conducted to determine the effect of modification straight blade angle by bending it inward and outward. Modified blade models with bend angle changes are shown in Figure 1. The diameter and distance between the blades of the five models are set equal to 40% of the chord length, and the bend angle varies from $\beta = 70^\circ$ to $\beta = 110^\circ$ with 10° intervals. Static and dynamic simulations are performed to observe turbine performance. Static simulations are performed to see the aerodynamic performance of the modified blades at various angular positions ($0^\circ - 150^\circ$, with interval 30°) to show some of the characteristic features of the flow around the turbine. For 180° to 360° positions are repeated (equal to 0° position) due to symmetrical blade shape, but there is a change of position between the advancing blade and the returning blade. Two parts of vortices produced at the advancing blade, one part is provided at the top of the tip of the advancing blade and moves downstream. The other part is built on the bottom of the tip of the advancing blade, which is divided into two ways: the first way runs along the concave side of the returning blade and the second way moves downstream. Thus there are two separation points. The vorticity influenced the average value of the drag coefficient and lift coefficient at different angle rotor positions.

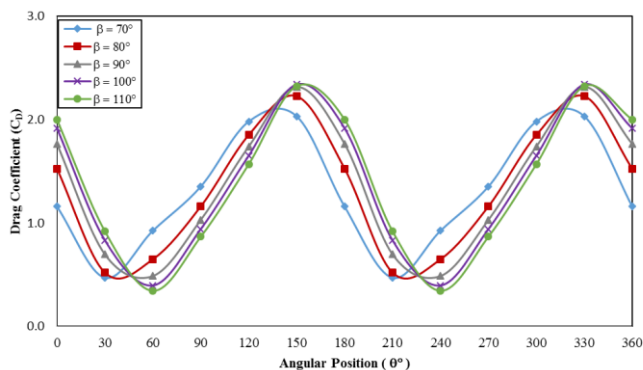


Figure 5: Drag coefficients at different angular position

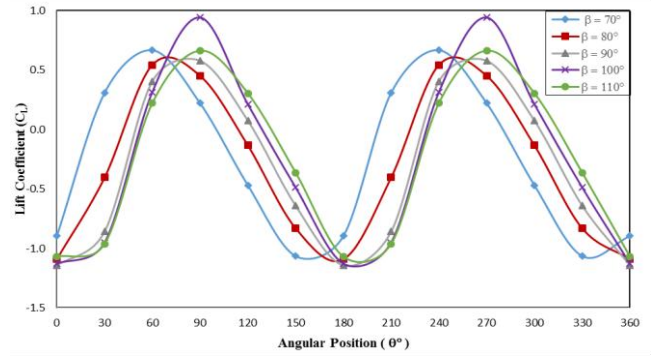


Figure 6: Lift coefficients at different angular position

Figure 5 shows that the drag coefficient (C_D) decreases from 0° to 60° angular positions and then gradually increases from 60° to 150° and then returns the same between the 180° position with the 0° position due to the symmetrical blade. A relatively high C_D value was obtained for a modified turbine at an angle bend position outward ($\beta = 100^\circ$ and 110°), compared to the other models. While Figure 6 shows the lift coefficient (C_L) value of the five-blade models. It is seen that the lift coefficient shows an increase from an angular position of 0° to 90° , and then decrease from 90° to 150° . This indicates that there are lift forces on the blade at the 60° and 90° positions. The negative lift coefficient occurs at 150° and 180° (same as 0° positions) as the acceleration of the returning blade moving into the flow creates a force in the clockwise direction. Thus the turbine does not operate purely with drag as the only contributing force, but in this case, lift force also contribute to increase power. The highest value of lift coefficient is obtained on bend angle $\beta = 100^\circ$ at a 90° and 270° positions.

3.3 Dynamic Simulations

Dynamic simulation is done by giving a specific rotational speed to the rotating zone. This study was made in the range of $TSR = 0.2$ to 1.4 . The value of the moment coefficient (C_M) and the power coefficient (C_P) is averaged over the time interval to see the performance ratios among the various proposed models.

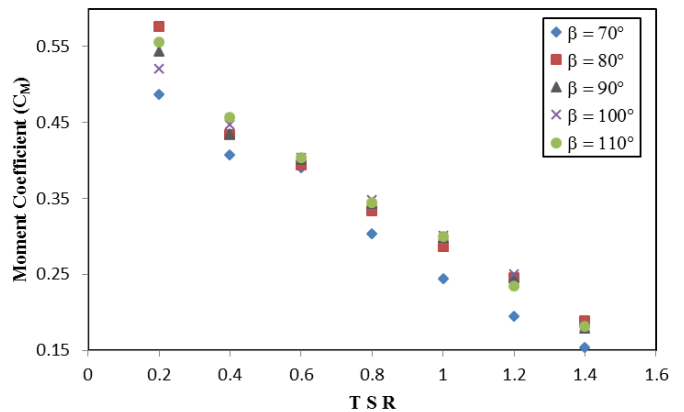


Figure 7: Moment coefficients at different TSRs

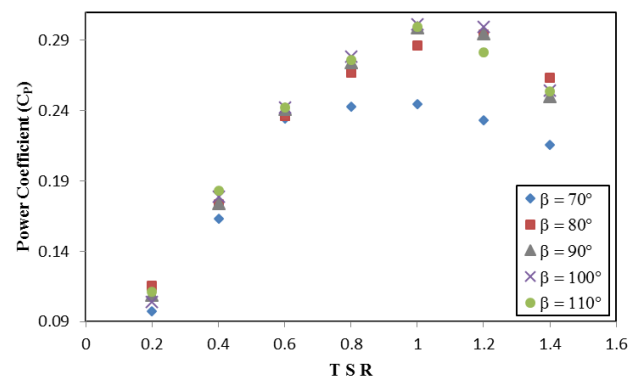


Figure 8: Power coefficients at different TSRs

Figure 7 and Figure 8 show the variation of moment coefficient and power coefficient for all models examined in this study. The average moment coefficient as a function of the tip speed ratio is presented in Figure 7. As it can be observed, the average value of the moment coefficient decreases approximately linearly as the tip speed ratio increases. The geometry design with $\beta = 80^\circ$ has the highest torque coefficient at lower tip speed ratios (TSR = 0.2), while at the higher tip speed ratios (TSR > 0.8) rotor with $\beta = 100^\circ$, the torque coefficient is the highest. Figure 8 presents a comparison of C_p characteristics for all the geometries. It can be seen that there are maximum value for each curve and the power coefficient increases with TSR up to a certain point after which it drops down as TSR further increases. All geometries attain maximum C_p at TSR = 1. In that TSR, the model with $\beta=100^\circ$ geometry produces the highest power output.

The Savonius turbine is a device that utilizes the drag force to gain power, but its performance is low due to the negative moment on the returning blade. Savonius blade with Bach type, the negative effect is significantly reduced due to backflow through the overlap region and the flow acceleration leading to the returning blade side. When the straight blade is bent inward ($\beta = 70^\circ$ and $\beta = 80^\circ$), the blade overlap distance becomes shorter than the baseline blade. On the other hand, the modification with the straight blade is bent outward ($\beta = 100^\circ$ and $\beta = 110^\circ$), the blade overlap distance becomes longer than the baseline blade. With the overlap distance too short, the return flow through this area is shorter than the overlap distance on the baseline blade, resulting in reduced aerodynamic performance. However, too long overlap distance can also decrease its performance, since the backflow time becomes longer and does not produce a positive effect on the returning blade. So in this case, the blade model with $\beta = 100^\circ$ generates the optimal distance, capable of maximizing the return flow over the overlap area, and giving the highest average power coefficient, $CP = 0.302$. To explain the flow physics around the Savonius wind rotor, the velocity contours between advancing blade and returning blade are plotted in Figure 9.

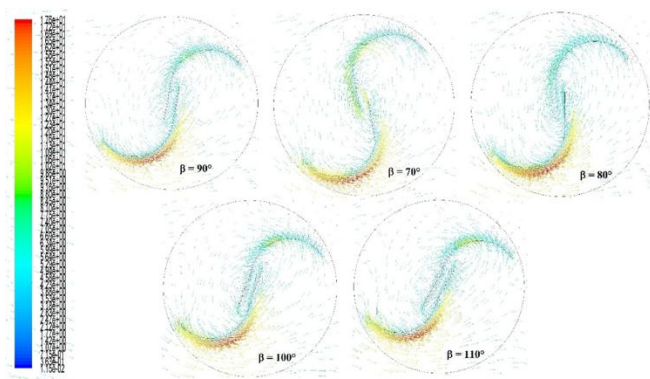


Figure 9: Velocity vector plots at various bend angle.

Figure 9 shows the difference of the velocity vector flow around the rotor of the five models tested: baseline (without bending or $\beta = 90^\circ$), bend inward ($\beta = 70^\circ$ and $\beta = 80^\circ$) and bend outward ($\beta = 100^\circ$ and $\beta = 110^\circ$). There are five flow conditions on the Savonius rotor: the free flow areas at the inlet, accelerating flow area at the rear edge of the returning blade, the overlap flow area between the blades, lifting flow on the convex of the advanced blade, and returning flow. The overlap flow area is the flow which provides a thrust effect on the advancing blades and the returning flow, where the stream is moved toward the concave side of the returning blade, helping to increase the torque of the rotor. With the same distance between blades and different at the overlap distance due to the effect of bending on the straight blade, the flow around the rotor causes the differences in the overlap area between the blades. This is due to the flow acceleration effect of continuing the thrust on the advancing blades. Beside that, the flow which provides the thrust on the advancing blade, is lower on the bending blades and the baseline blades related to short overlap spacing. However, with higher overlap spacing due to larger bend angle ($\beta = 110^\circ$), it can contribute to cause a blockage effect so that the return flow toward the concave side is inhibited, which causes its performance to decline. Thus the optimum blade design is obtained at the outward bending blade of $\beta = 100^\circ$.

4. CONCLUSIONS

This study presents numerical investigation to simulate and verify the effect of the straight blade angle on the performance of the modified Bach-type of Savonius wind turbine. There are five turbine models including baseline model (without bending at the point of the curve and straight blade or $\beta=90^\circ$), two models bent inwards ($\beta=70^\circ$ and $\beta=80^\circ$), and two models bent outwards ($\beta=100^\circ$ and $\beta=110^\circ$). Both the static and dynamic

simulations were performed using 2D CFD Fluent. In the static simulation, the drag and lift coefficient on the Savonius turbine were directly calculated at every angular position. From static simulations, it has been observed that a relatively high CD value was obtained for a modified turbine at an angle bend position outward ($\beta = 100^\circ$ and 110°) and the highest value of lift coefficient is obtained on bend angle $\beta = 100^\circ$ at a 90° and 270° positions, compared to the other models. Furthermore, the dynamic two-dimensional simulation data have been collected at different tip speed ratio values, and the results show that the rotor with a straight blade angle of $\beta = 100^\circ$ has the highest coefficient of power, 0.302, for the tip speed ratio 1, which is 0.84% higher than a baseline model, and the rotor with a straight blade angle of $\beta = 70^\circ$ has the lowest coefficient of power, 0.244, for the tip speed ratio 1.

REFERENCES

- [1] Vani, R.S., Mutalikdesai, S.B., Kumar, A. 2017. Design and Fabrication of Vertical Axis Wind Turbine for Water Pump Application. *Journal of Mechanical Engineering and Automation*, 7 (4), 95–98.
- [2] Zingman, A. 2007. Optimization of a Savonius Rotor Vertical-Axis Wind Turbine for Use in Water Pumping Systems in Rural Honduras. Undergraduate Thesis, Massachusetts Institute of Technology, Dept. of Mechanical Engineering.
- [3] Riccii, R., Romagnoli, R., Montelpare, S., Vitali, D. 2016. Experimental study on a Savonius wind rotor for street lighting systems. *Applied Energy*, 161, 143–152.
- [4] Menet, J.L. 2004. A double-step Savonius rotor for local production of electricity: a design study. *Renewable Energy*, 29, 1843–1862.
- [5] Mao, Z., Tian, W. 2015. Effect of the blade arc angle on the performance of a Savonius wind turbine. *Advances in Mechanical Engineering*, 7 (5), 1–10.
- [6] Roy, S., Saha, U.K. 2013. Investigations on The Effect Of Aspect Ratio Into The Performance Of Savonius Rotors. *Proceedings of the ASME 2013 Gas Turbine India Conference*, 1–6.
- [7] Jaohindy, P., McTavish, S., Garde, F., Bastide, A. 2013. An analysis of the transient forces acting on Savonius rotors with different aspect ratios. *Renewable Energy*, 55, 286–295.
- [8] Akwa, J.V., Gilmar Alves da Silva, J., Petry, A.P. 2012. Discussion on the verification of the overlap ratio influence on performance coefficients of a Savonius wind rotor using computational fluid dynamics. *Renewable Energy*, 38, 141–149.
- [9] Abbaszadeh, M., Bagherzadeh, F., Irvani, M. 2012. A numerical investigation to study effects of a savonius rotor's Plate shape on its optimum overlap ratio. *Proceedings of the ASME 2012 Gas Turbine India Conference*, 253–258.
- [10] Abbaszadeh, M., Doroodian, F. 2012. A numerical investigation on effects of the gap between plates of Savonius vertical axis wind turbines with different shapes on their performance. *Proceedings of the ASME 2012 Gas Turbine India Conference*, 259–264.
- [11] Wenehenubun, F., Saputra, A., Sutanto, H. 2015. An experimental study on the performance of Savonius wind turbines related with the number of blades. *Energy Procedia*, 68, 297 – 304.
- [12] Emmanuel, B., Jun, W. 2011. Numerical Study of a Six-Bladed Savonius Wind Turbine. *Journal of Solar Energy Engineering*, 133, 044503-1-5.
- [13] Baz, A.M., Mahmoud, N.A., Hamed, A.M., Youssef, K.M. 2015. Optimization Of Two And Three Rotor Savonius Wind Turbine. *Proceedings of ASME Turbo Expo 2015: Turbine Technical Conference and Exposition*.
- [14] Rahman, M., Morshed, K.N., Lewis, J., Fuller, M. 2009. Experimental and Numerical Investigations On Drag And Torque Characteristics Of Three-Bladed Savonius Wind Turbine. *Proceedings of the ASME 2009 International Mechanical Engineering Congress & Exposition*, 85–94.
- [15] Kamoji, M.A., Kedare, S.B., Prabhu, S.V. 2011. Experimental Investigations on Two and Three Stage Modified Savonius Rotor. *Wind Engineering*, 35 (4), 483–510.

- [16] Frikha, S., Driss, Z., Ayadi, E., Masmoudi, Z., Abid, M.S. 2016. Numerical and experimental characterization of multi-stage Savonius rotors. *Energy*, 114, 382–404.
- [17] Altan, B.D., Atılgan, M. 2012. A study on increasing the performance of Savonius wind rotors. *Journal of Mechanical Science and Technology*, 26 (5), 1493–1499.
- [18] Roy, S., Saha, U.K. 2014. Performance Analysis Of Savonius-Style Wind Turbines Under Concentrated And Oriented Jets. *Proceedings of ASME Turbo Expo 2014: Turbine Technical Conference and Exposition*, pp. 1–7.
- [19] El Baz, A.M., Mahmoud, N.A. 2015. Numerical modelling of savonius wind turbine with downstream baffle. *Proceedings of ASME Turbo Expo 2015: Turbine Technical Conference and Exposition*.
- [20] Mohamed, M.H., Janiga, G., Pap, E., Thévenin, D. 2011. Optimal blade shape of a modified Savonius turbine using an obstacle shielding the returning blade. *Energy Conversion and Management*, 52, 236–242.
- [21] Korprasertsak, N., Leephakpreeda, T. 2015. CFD-Based Power Analysis on Low Speed Vertical Axis Wind Turbines with Wind Boosters. *Energy Procedia*, 79, 963 – 968.
- [22] El-Askary, W.A., Nasef, M.H., EL-hamid, A.A.A., Gad, H.E. 2015. Harvesting wind energy for improving performance of Savonius rotor. *Journal of Wind Engineering and Industrial Aerodynamics*, 139, 8–15.
- [23] Driss, Z., Mlayeh, O., Driss, D., Maaloul, M., Abid, M.S. 2014. Numerical simulation and experimental validation of the turbulent flow around a small incurved Savonius wind rotor. *Energy*, 74, 506e517.
- [24] Sharma, S., Sharma, R.K. 2016. Performance improvement of Savonius rotor using multiple quarter blades – A CFD investigation. *Energy Conversion and Management*, 127, 43–54.
- [25] Al-Faruk, A., Sharifian, A. 2016. Geometrical optimization of a swirling Savonius wind turbine using an open jet wind tunnel. *Alexandria Engineering Journal*, 55, 2055–2064.
- [26] Anbarsooz, M. 2016. Aerodynamic performance of helical Savonius wind rotors with 30° and 45° twist angles. *Experimental and numerical studies*. *Journal of Power and Energy*, 1–12.
- [27] Sanusi, A., Soeparman, S., Wahyudi, S., Yuliati, L. 2016. Experimental Study of Combined Blade Savonius Wind Turbine. *International Journal of Renewable Energy Research*, 6 (2), 614–619.
- [28] Salyers, T.E. 2016. Experimental and Numerical Investigation of Aerodynamic Performance for Vertical-Axis Wind Turbine Models with Various Blade Designs. *Electronic Theses & Dissertations Paper 1418*, Georgia Southern University, Georgia.
- [29] Modi, V.J., Fernando, F.S.U.K. 1989. On the Performance of the Savonius Wind Turbine. *Journal of Solar Energy Engineering*, 111, 71–81.
- [30] Kamoji, M.A., Kedare, S.B., Prabhu, S.V. 2009. Experimental investigations on single stage modified Savonius rotor. *Applied Energy*, 86, 1064–1073.
- [31] Wang, L., Yeung, R.W. 2016. On the performance of a micro-scale Bach-type turbine as predicted by discrete-vortex simulations. *Applied Energy*, 183, 823–836.
- [32] Alom, N., Borah, B., Saha, U.K. 2018. An insight into the drag and lift characteristics of modified Bach and Benesh profiles of Savonius rotor. *Energy Procedia*, 144, 50–56.
- [33] Kacprzak, K., Liskiewicz, G., Sobczak, K. 2013. Numerical investigation of conventional and modified Savonius wind turbines. *Renewable Energy*, 60, 578–585.
- [34] Roy, S., Saha, U.K. 2013. Numerical Investigation to Assess an Optimal Blade Profile for The Drag Based Vertical Axis Wind Turbine. *Proceedings of the ASME 2013 International Mechanical Engineering Congress and Exposition*, San Diego, California, USA.
- [35] Blackwell, B.F., Sheldahl, R.E., Feltz, L.V. 1977. *Wind Tunnel Performance Data for Two and Three-Bucket Savonius Rotors*. Sandia Laboratories, Albuquerque, New Mexico, Unlimited Release SAND76-0131.
- [36] Sheikh, H.M., Shabbir, Z., Ahmed, H., Waseemh, M.H., Sheikh, M.Z. 2017. Computational fluid dynamics analysis of a modified Savonius rotor and optimization using response surface methodology. *Wind Engineering*, 41 (5), 1–12.

